Journal of Southeast University (English Edition) Vol. 21, No. 1, pp. 97 - 101 Mar. 2005 ISSN 1003—7985

Meso-mechanical analyses of shape memory alloy wires reinforced smart structures with damages

Hu Zili Zhou Wanlin

(Aeronautical Science Key Laboratory for Smart Materials and Structures,
Nanjing University of Aeronautics and Astronautics, Nanjing 210016, China)

Abstract: The thermo-mechanical behaviors of shape memory alloy (SMA) wires reinforced smart structures with damages are analyzed through variational principle and meso-mechanical method. A governing equation on the structure is derived. Mathematical expressions on meso-displacement field, stress-strain field of typical element with damages are presented. A failure criterion for interface failure between SMA wires and matrix is established under two kinds of actuation which are dead-load and temperature, where the temperature is included in effective free restoring strain. In addition, there are some other composing factors in the failure criterion such as interface properties, thermodynamical properties of SMA, initial debonding length $L-l$, etc. The results are significant to understand structural strength self-adaptive control and failure mechanism of SMA wires reinforced smart structures with damages, and provide a theoretical foundation for further study on the integrity of SMA smart structures.

Key words: smart structure; damage; shape memory alloy; failure; meso-mechanical analysis; variational principle

Smart structures have attracted more and more attention due to their dual properties of conventional composite structures and functional composite structures. They are being applied or to be applied in some fields, such as aeronautics and astronautics, national defense, architecture, and medicine[1-4]. Among them, shape memory alloy (SMA) reinforced smart structures could be used to do self-adaptive structural shape and strength and to prevent structural failures. Although many researches on SMA reinforced smart structures without damages have been made[5-11]; researches on SMA smart structures with damages have rarely reported thus far[12,13]. In this paper, thermo-mechanical behaviors of SMA wires reinforced smart structures with damages have been analyzed by utilizing a variational principle. The results presented herein provide a theoretical basis for further study on the integrity of SMA smart structures.

There are three restoring states of SMA wires in smart structures; they are free restoring, restrained restoring, and controlled restoring. Considering a controlled restoring state, which is similar to an actual situation, a one-dimensional constitutive relation of SMA can be written as

$$\varepsilon_{\mathrm{r}} = \varepsilon - \varepsilon_{\mathrm{res}} = k_1\sigma + k_2 \tag{1}$$

where ε_{r}, ε and $\varepsilon_{\mathrm{res}}$ are the restoring strain, total strain and pre-strain, respectively; k_1 and k_2 are the effective restoring flexibility and effective free restoring strain, respectively.

1 Analysis Model and Typical Element

Assume that analysis object is SMA reinforced one-directional composites, and partial failures of interface at the ends have taken place, but there are still bridge and friction effects between peeled faces, which resist peeling damage development. We use equivalent friction shear stress τ_{p} to denote the degree of resistance effect, and assume that

$$\tau_{\mathrm{p}} = \tau_0 \frac{l}{L} \tag{2}$$

Received 2004-03-31.

Foundation items: The Aeronautical Science Foundation of China (No. 01G52041), the National Natural Science Foundation of China (No. 10072026, 50135030).

Biography: Hu Zili (1964—), male, doctor, associate researcher, huzlgp@163.com.

where τ_0 denotes instantaneous equivalent friction shear stress just after initial peeling, and $0 \leqslant \tau_0 \leqslant \tau_b$ (when $l = L$, $\tau_0 = \tau_b$), τ_b is the shear yield strength of the interface.

The typical element of an SMA reinforced smart structure with damages is shown in Fig. 1, where L is the half length of the element, l is the length of a portion without damage, $L - l$ is the length of a peeled portion, r_f is the radius of the SMA wire, and r is the radius of any circle round matrix. Let R denote the maximum radius of circle round matrix, and define ε_0 ($\varepsilon_0 = \partial w_R / \partial z$) as the known average strain of an SMA reinforced smart structure. P_a is a concentrating load at ends of the SMA wire, and there is an equation $P_a = \pi r_f^2 \sigma_a$, where σ_a denotes the average stress at ends of the SMA wire.

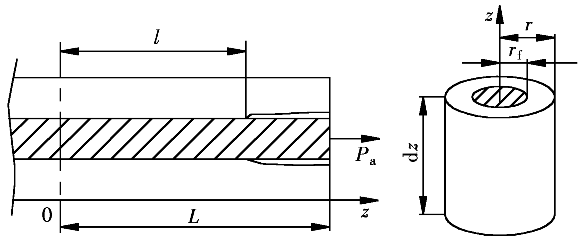

Fig. 1 Typical element of SMA reinforced smart structure with damages

2 Variational Principle on Failure of SMA Reinforced Smart Structure with Damages

We just consider a half of a typical element because of symmetry, the strain energy u_e of typical element is composed of the tensile strain energy u_f of SMA wire and the shearing strain energy u_m of matrix. Therefore, there is

$$u_e = u_f + u_m \tag{3}$$

where

$$u_f = \int_V \frac{1}{2} \sigma_f \varepsilon_f \mathrm{d}V \tag{4}$$

$$u_m = \frac{1}{2G_m} \int_V \tau^2 \mathrm{d}V = \frac{1}{2G_m} \int_0^l \int_0^{2\pi} \int_{r_f}^R \left(\frac{r_f}{r} \tau_i \right)^2 r \mathrm{d}r \mathrm{d}\theta \mathrm{d}z + \frac{1}{2G_m} \int_l^L \int_0^{2\pi} \int_{r_f}^R \left(\frac{r_f}{r} \tau_p \right)^2 r \mathrm{d}r \mathrm{d}\theta \mathrm{d}z = \frac{\pi r_f^2 \ln(R/r_f)}{G_m} \int_0^l \tau_i^2 \mathrm{d}z + \frac{\pi r_f^2 \ln(R/r_f)}{G_m} \int_l^L \tau_p^2 \mathrm{d}z \tag{5}$$

where τ_i is the interface shear stress. Considering a situation of slight deformation, we have[13]

$$\tau_i = \frac{G_m (w_R - w_f)}{r_f \ln(R/r_f)} \tag{6}$$

where w_f is the axial displacement of SMA wire at $r = r_f$, and w_R is the axial displacement of matrix at $r = R$.

Substituting Eq. (1) into Eq. (4) and noting that $\frac{\mathrm{d}w_f}{\mathrm{d}z} = \varepsilon_f = \varepsilon_r$, we can obtain

$$u_f = \frac{\pi r_f^2}{2k_1} \int_0^L \left[\left(\frac{\mathrm{d}w_f}{\mathrm{d}z} \right)^2 - k_2 \frac{\mathrm{d}w_f}{\mathrm{d}z} \right] \mathrm{d}z \tag{7}$$

Introducing Eq. (6) into Eq. (5), we have

$$u_m = \frac{\pi G_m}{\ln(R/r_f)} \int_0^l (w_R - w_f)^2 \mathrm{d}z + \frac{\pi r_f^2 \ln(R/r_f)}{G_m} \tau_p^2 (L - l) \tag{8}$$

Thus, the function of potential energy can be expressed as

$$\Pi_e = 2\left(u_f + u_m - P_a w_f(L) + \int_l^L f_p w_f \mathrm{d}z \right) \tag{9}$$

where f_p is the equivalent friction shear stress of the peeled portion in a unit of length, and there is $f_p = 2\pi r_f \tau_p$.

According to the principle of action of minimum potential energy[14, 15], the first variation of the function of potential energy is equal to zero, that is

$$\delta \Pi_e [w_f(z)] = 0 \tag{10}$$

Then, we can obtain

$$\frac{\pi r_f^2}{2k_1} \int_0^L \left(2 \frac{\mathrm{d}w_f}{\mathrm{d}z} \frac{\mathrm{d}\delta w_f}{\mathrm{d}z} - k_2 \frac{\mathrm{d}\delta w_f}{\mathrm{d}z} \right) \mathrm{d}z + \frac{\pi G_m}{\ln(R/r_f)} \int_0^l 2(w_R - w_f)(\delta w_R - \delta w_f) \mathrm{d}z - P_a \delta w_f \big|_L + \int_l^L f_p \delta w_f \mathrm{d}z = 0 \tag{11}$$

To integrate the first item of Eq. (11) in subsection, noting that $\delta w_R = 0$ (where w_R has been defined as the known displacement), then we have

$$\frac{\pi r_f^2}{k_1} \left(\frac{\mathrm{d}w_f}{\mathrm{d}z} \delta w_f \bigg|_0^L - \int_0^L \delta w_f \frac{\mathrm{d}^2 w_f}{\mathrm{d}z^2} \mathrm{d}z \right) - \frac{k_2 \pi r_f^2}{2k_1} \delta w_f \bigg|_0^L + \frac{\pi G_m}{\ln(R/r_f)} \int_0^l 2(w_R - w_f)(-\delta w_f) \mathrm{d}z - P_a \delta w_f \big|_L + \int_l^L f_p \delta w_f \mathrm{d}z = 0 \tag{12}$$

Because of $\delta w_{\mathrm{f}}(0)=0$, Eq. (12) can be rewritten as

$$\left(\frac{\pi r_{\mathrm{f}}^2}{k_1}\frac{\mathrm{d}w_{\mathrm{f}}}{\mathrm{d}z}\bigg|_L-\frac{k_2\pi r_{\mathrm{f}}^2}{2k_1}-P_{\mathrm{a}}\right)\delta w_{\mathrm{f}}\bigg|_L-\frac{\pi r_{\mathrm{f}}^2}{k_1}\int_0^L\frac{\mathrm{d}^2 w_{\mathrm{f}}}{\mathrm{d}z^2}\delta w_{\mathrm{f}}\mathrm{d}z-\frac{2\pi G_{\mathrm{m}}}{\ln(R/r_{\mathrm{f}})}\int_0^l(w_{\mathrm{R}}-w_{\mathrm{f}})\delta w_{\mathrm{f}}\mathrm{d}z+\int_l^L f_{\mathrm{p}}\delta w_{\mathrm{f}}\mathrm{d}z=0 \quad (13)$$

Now we introduce a function as follows:

$$\langle z-l\rangle=\begin{cases}1 & 0\leqslant z\leqslant l\\ 0 & l<z\leqslant L\end{cases} \quad (14)$$

The domain of definition of the function is $[0, L]$.

Thus, Eq. (13) becomes

$$\left(\frac{\pi r_{\mathrm{f}}^2}{k_1}\frac{\mathrm{d}w_{\mathrm{f}}}{\mathrm{d}z}\bigg|_L-\frac{k_2\pi r_{\mathrm{f}}^2}{2k_1}-P_{\mathrm{a}}\right)\delta w_{\mathrm{f}}\bigg|_L-\frac{\pi r_{\mathrm{f}}^2}{k_1}\int_0^L\frac{\mathrm{d}^2 w_{\mathrm{f}}}{\mathrm{d}z^2}\delta w_{\mathrm{f}}\mathrm{d}z-\frac{2\pi G_m}{ln(\mathrm{R}/\mathrm{r}_f)}\int_0^{\mathrm{L}}(\mathrm{w}_R-\mathrm{w}_f)\langle \mathrm{z}-\mathrm{l}\rangle\delta\mathrm{w}_f dz+\int_0^L f_{\mathrm{p}}(1-\langle z-l\rangle)\delta w_{\mathrm{f}}\mathrm{d}z=0 \quad (15)$$

To any slight virtual displacement, the first item of Eq. (15) gives out boundary condition:

$$\frac{\pi r_{\mathrm{f}}^2}{k_1}\frac{\mathrm{d}w_{\mathrm{f}}}{\mathrm{d}z}\bigg|_L-\frac{k_2\pi r_{\mathrm{f}}^2}{2k_1}-P_{\mathrm{a}}=0 \quad (16)$$

And other items give out governing equation:

$$-\frac{\pi r_{\mathrm{f}}^2}{k_1}\frac{\mathrm{d}^2 w_{\mathrm{f}}}{\mathrm{d}z^2}-\frac{2\pi G_{\mathrm{m}}}{\ln(R/r_{\mathrm{f}})}(w_{\mathrm{R}}-w_{\mathrm{f}})\langle z-l\rangle+f_{\mathrm{p}}(1-\langle z-l\rangle)=0 \quad (17)$$

Expressing Eq. (17) in different portions and solving it, in a portion $0\leqslant z\leqslant l$, there is

$$-\frac{\pi r_{\mathrm{f}}^2}{k_1}\frac{\mathrm{d}^2 w_{\mathrm{f}}}{\mathrm{d}z^2}-\frac{2\pi G_{\mathrm{m}}}{\ln(R/r_{\mathrm{f}})}(w_{\mathrm{R}}-w_{\mathrm{f}})=0 \quad (18)$$

Let $n^2=\dfrac{2k_1 G_{\mathrm{m}}}{r_{\mathrm{f}}^2\ln(R/r_{\mathrm{f}})}$, and note that $w_{\mathrm{R}}=\varepsilon_0 z$, then Eq. (18) can be written as

$$\frac{\mathrm{d}^2 w_{\mathrm{f}}}{\mathrm{d}z^2}+n^2(\varepsilon_0 z-w_{\mathrm{f}})=0 \quad (19)$$

The solution of Eq. (19) is

$$w_{\mathrm{f}}(z)=\frac{C_1}{n}\cosh(nz)+\frac{C_2}{n}\sinh(nz)+\varepsilon_0 z+C_3 \quad (20)$$

where C_1, C_2 and C_3 are the coefficients to be determined.

In a portion $l<z\leqslant L$, there exists

$$-\frac{\pi r_{\mathrm{f}}^2}{k_1}\frac{\mathrm{d}^2 w_{\mathrm{fp}}}{\mathrm{d}z^2}+f_{\mathrm{p}}=0 \quad (21)$$

where w_{fp} denotes the displacement of SMA wire in the peeled portion. The solution of Eq. (21) is

$$w_{\mathrm{fp}}=\frac{k_1\tau_{\mathrm{p}}}{r_{\mathrm{f}}}z^2+C_4 z+C_5 \quad (22)$$

where C_4 and C_5 are coefficients to be determined. In addition to boundary condition Eq. (16) there are four other boundary conditions as follows:

$$w_{\mathrm{f}}\big|_0=0,\ w_{\mathrm{f}}\big|_l=w_{\mathrm{fp}}\big|_l,\ \frac{\mathrm{d}w_{\mathrm{f}}}{\mathrm{d}z}\bigg|_l=\frac{\mathrm{d}w_{\mathrm{fp}}}{\mathrm{d}z}\bigg|_l,\ \ \tau_{\mathrm{p}}=\frac{G_{\mathrm{m}}(w_{\mathrm{R}}-w_{\mathrm{fp}})}{r_{\mathrm{f}}\ln(R/r_{\mathrm{f}})} \quad (23)$$

Therefore we can establish coupled equations of the coefficients through Eqs. (16), (22) and (23).

$$\left.\begin{aligned}
&\frac{C_1}{n}+C_3=0\\
&C_1\sinh(nl)+C_2\cosh(nl)+\varepsilon_0=\frac{2k_1\tau_{\mathrm{p}}l}{r_{\mathrm{f}}}+C_4\\
&\frac{C_1}{n}\cosh(nl)+\frac{C_2}{n}\sinh(nl)+\varepsilon_0 l+C_3=\frac{k_1\tau_{\mathrm{p}}}{r_{\mathrm{f}}}l^2+C_4 l+C_5\\
&\frac{\pi r_{\mathrm{f}}^2}{k_1}\left(\frac{2k_1\tau_{\mathrm{p}}}{r_{\mathrm{f}}}L+C_4\right)-\frac{k_2\pi r_{\mathrm{f}}^2}{2k_1}-P_{\mathrm{a}}=0\\
&\varepsilon_0 z\Big|_L-\frac{\tau_{\mathrm{p}}r_{\mathrm{f}}\ln(R/r_{\mathrm{f}})}{G_{\mathrm{m}}}=\frac{k_1\tau_{\mathrm{p}}}{r_{\mathrm{f}}}z^2\Big|_L+C_4 z\Big|_L+C_5
\end{aligned}\right\} \quad (24)$$

Solutions of the above coupled equations are

$$C_4 = \frac{k_2}{2} + \sigma_a k_1 - \frac{2k_1\tau_0 l}{r_f} \tag{25}$$

$$C_5 = \left(\varepsilon_0 - \frac{k_2}{2} - \sigma_a k_1\right)L - \frac{\tau_0 l r_f \ln(R/r_f)}{G_m L} + \frac{k_1\tau_0 L l}{r_f} \tag{26}$$

$$C_1 = \frac{\varepsilon_0\sinh(nl) - n\varepsilon_0 l\cosh(nl)}{1-\cosh(nl)} + \frac{k_1\tau_0 l^2[nl\cosh(nl) - 2\sinh(nl)]}{[1-\cosh(nl)]Lr_f} + \frac{nl\cosh(nl) - \sinh(nl)}{1-\cosh(nl)}C_4 + \frac{n\cosh(nl)}{1-\cosh(nl)}C_5 \tag{27}$$

$$C_2 = \frac{2k_1\tau_0 l^2}{Lr_f\cosh(nl)} + \frac{C_4}{\cosh(nl)} - \frac{\varepsilon_0}{\cosh(nl)} - \frac{C_1\sinh(nl)}{\cosh(nl)} \tag{28}$$

$$C_3 = -\frac{C_1}{n} \tag{29}$$

Substituting Eq. (20) into Eq. (6), we can get the shear stress of interface between SMA wire and matrix in the portion $0 \leqslant z \leqslant l$

$$\tau_i = \frac{G_m\left[-\frac{C_1}{n}\cosh(nz) - \frac{C_2}{n}\sinh(nz) - C_3\right]}{r_f\ln\left(\frac{R}{r_f}\right)} \tag{30}$$

3 A Criterion of Interface Failure for SMA Reinforced Smart Structure with Damages

Substituting C_1, C_2 and C_3 into Eq. (30) and solving the maximum shear stress of the interface, we get

$$\tau_{\mathrm{imax}} = \frac{k_1 G_m(L-l)}{r_f\ln(R/r_f)}\left[\sigma_a - \frac{\tau_0 l(L-l)}{Lr_f} - \frac{\varepsilon_0}{k_1} + \frac{k_2}{2k_1}\right] + \frac{\tau_0 l}{L} \tag{31}$$

When τ_{imax} achieves the shear strength τ_b of the interface, the interface failure takes place. Therefore, a criterion of the interface failure for SMA reinforced smart structure with damages can be established as

$$\tau_{\mathrm{imax}} \leqslant \tau_b \tag{32}$$

Eq. (32) actually consists of two kinds of actuation which are dead-load and temperature, where the temperature is included in parameter k_2. It is not difficult to find that there are many composing factors in the failure criterion for interface failure. They are interface properties, dead-load, temperature, thermodynamical properties of SMA, initial debonding length $L-l$, etc. If let $\tau_{\mathrm{imax}} = \tau_b$, then the stress σ_a is defined as debonding stress, and denoted by σ_{aT},

$$\sigma_{aT} = \frac{r_f\ln(R/r_f)(\tau_b L - \tau_0 l)}{k_1 G_m L(L-l)} + \frac{\tau_0 l(L-l)}{Lr_f} + \frac{\varepsilon_0}{k_1} - \frac{k_2}{2k_1} \tag{33}$$

In terms of Eq. (33), we can obtain the debonding stress of the interface under two kinds of actuation which are dead-load and temperature.

4 Conclusions

1) Thermo-mechanical behaviors of SMA wires reinforced smart structures with damages have been analyzed through variational principle and meso-mechanical method, mathematical expressions on meso-displacement field, stress-strain field of typical element with damages have been presented.

2) The criterion of interface failure for SMA wires reinforced smart structures with damages has been established under two kinds of actuation which are dead-load and temperature, where the temperature is included in parameter k_2. In addition, there are some other composing factors in the failure criterion, such as interface properties, thermodynamical properties of SMA, initial debonding length $L-l$, etc.

References

[1] Liberatore S, Carman G P. Damage detection of structures based on spectral methods using piezoelectric materials [A]. In: *Structural Health Monitoring* [C]. CRC Press, 2003, **1**: 606 - 614.

[2] Dolye C, Staveley C, Henderson P. Structural health monitoring using optical fibre strain sensing systems [A]. In: *Structural Health Monitoring* [C]. CRC Press, 2003, **1**: 944 - 951.

[3] Park G, Inman D J, Farrar C R. Recent studies in piezoelectric impedance-based structural health monitoring [A]. In: *Structural Health Monitoring* [C]. CRC Press, 2003, **1**: 1423 - 1430.

[4] Tao Baoqi. *Smart materials and structures* [M]. Beijing: National Defense Industry Press, 1997. (in Chinese)

[5] Furuya Yasubumi. Design and material evaluation of shape memory composites [J]. *Journal of Intelligent Material Systems and Structures*, 1996, **7**(3): 321 - 330.

[6] Stalmans R, Delaey L, Van Humbeeck J. Modeling of adaptive composite materials with embedded shape memory alloy wires [A]. In: *Materials Research Society Symposium Proceedings* [C]. Boston, 1997, **459**: 119 - 130.

[7] Wei Z G, Sandstrom R, Miyazaki S. Shape memory materials and hybrid composites for smart systems, Part Ⅱ: Shape-memory hybrid composites[J]. *Journal of Materials Science*, 1998, **33**(15): 3763 - 3783.

[8] Song Guquan, Sun Qingping, Cherkaoui M. Role of microstructure in the thermomechanical behaviour of SMA composites [J]. *Transactions of the ASME*, 1999, **121**(1): 86 - 92.

[9] Birman V. Review of mechanics of shape memory alloy structures [J]. *Applied Mechanics Review*, 1997, **50**(11): 629 - 645.

[10] Boyd G, Lagoudas D C. A thermodynamical constitutive model for shape memory materials, Part Ⅱ: The SMA composite material [J]. *Int J Plasticity*, 1996, **12**(7): 843 - 873.

[11] Bo Z, Lagoudas D C. Thermomechanical modeling of polycrystalline SMAs under cyclic loading, Part Ⅰ: Theoretical derivations[J]. *International Journal of Engineering Science*, 1999, **37**(9): 1089 - 1140.

[12] Hu Zili, Xiong Ke, Wang Xinwei. One-dimensional incremental constitutive relation of SMA fiber reinforced smart composites with damages [J]. *Transactions of Nanjing University of Aeronautics and Astronautics*, 2003, **35**(5): 465 - 473. (in Chinese)

[13] Hu Zili. Properties characterization and meso-mechanical analysis of smart structures with damages [D]. Nanjing: Institute of Unmanned Aerocraft of Nanjing University of Aeronautics and Astronautics, 2003. (in Chinese)

[14] Li Jingyong. *Finite element method* [M]. Beijing: Beijing University of Posts and Telecommunications Press, 2000. (in Chinese)

[15] Hu Haichang. *Variational principle and application of elasticity* [M]. Beijing: Science Press, 1982. (in Chinese)

含损伤形状记忆合金增强智能结构的细观分析

胡自力　　周晚林

(南京航空航天大学智能材料与结构航空科技重点实验室, 南京 210016)

摘要: 从细观角度出发, 运用变分原理对含损伤形状记忆合金(SMA)增强智能结构的热、力学行为进行了分析, 导出了含损伤 SMA 增强智能结构的控制方程, 给出了含损伤典型单元体的细观位移场、应力应变场的数学描述, 建立了 SMA 增强智能结构的界面失效判据. 在界面失效判据中, 不仅包含了力载荷和温度载荷 2 种激励, 其中温度激励隐含在有效自由回复应变当中, 还包含了界面性能、SMA 热力学性能、界面初始脱粘长度等因素. 这些结果对认识含损伤 SMA 增强智能结构的强度自适应控制及其失效机理有一定意义, 同时为进一步研究智能结构的完整性提供了相应的理论支持.

关键词: 智能结构; 损伤; 形状记忆合金; 失效; 细观分析; 变分原理

中图分类号: TB330. 1; TB381